Prediction of CW chord as a measure for the eye's orientation axis after cataract surgery from preoperative IOLMaster 700 measurement data

Achim Langenbucher,[1] Nóra Szentmáry,[2,3] Alan Cayless,[4] Johannes Weisensee,[1] Jascha Wendelstein[5] and Peter Hoffmann[6]

[1]Department of Experimental Ophthalmology, Saarland University, Homburg/Saar, Germany
[2]Dr. Rolf M. Schwiete Center for Limbal Stem Cell and Aniridia Research, Saarland University, Homburg/Saar, Germany
[3]Department of Ophthalmology, Semmelweis-University, Budapest, Hungary
[4]School of Physical Sciences, The Open University, Milton Keynes, UK
[5]Department of Ophthalmology, Johannes Kepler University Linz, Linz, Austria
[6]Augen- und Laserklinik Castrop-Rauxel, Castrop-Rauxel, Germany

ABSTRACT.

Background: The angles alpha and kappa are widely discussed for centring refractive procedures, but they cannot be determined with ophthalmic instruments. The purpose of this study is to investigate the Chang-Waring chord (position of the Purkinje reflex PI relative to the corneal centre) derived from an optical biometer before and after cataract surgery and to study the changes resulting from cataract surgery.

Methods: The analysis was based on a large dataset of 1587 complete sets of preoperative and postoperative IOMaster 700 biometry measurements from two clinical centres, each containing: valid data for pupil and corneal centre position, the position of the Purkinje reflex PI originated from a coaxial fixation target, keratometry (K), axial length (AL), anterior chamber depth (ACD), lens thickness (LT), central corneal thickness CCT, and horizontal corneal diameter W2W. The Chang-Waring chord CW was derived from pupil centre and Purkinje reflex PI analysed preoperatively and postoperatively, and a multilinear regression model together with a feedforward neural network algorithm was set up to predict postoperative CW chord from preoperative CW chord, K and biometric distances of the eye.

Results: The Y component of CW chord shows a slight shift in the inferior direction in both left and right eyes, before and after cataract surgery. The X component shows some shift in the temporal direction, which is more pronounced preoperatively and slightly reduced postoperatively but with a larger variation. The change in CW chord from preoperative to postoperative shows a slight shift in the superior and nasal directions. Our algorithms for prediction of postoperative CW chord using preoperative CW chord, keratometry and biometry as input data performed with a multilinear regression and a feedforward neural network approach were able to reduce the variance, but could not properly predict the postoperative CW chord X and Y components.

Conclusion: The CW chord as the position of the Purkinje reflex PI with respect to the pupil centre can be directly measured with any biometer, topographer or tomographer with a coaxial fixation light. The mean Y component does not differ between right and left eyes or preoperatively and postoperatively, but the mean temporal shift of the X component preoperatively is slightly reduced postoperatively, but with a larger scatter of the values.

Key words: angle alpha – angle kappa – biometry – cataract – Chang-Waring chord – deep learning – feedforward multi-output network – multilinear regression

Background

In the last two decades, the angles alpha and kappa have been widely discussed as predictors for the visual performance after cataract surgery or corneal refractive surgery (Arba Mosquera et al. 2015; Barragán-Garza et al. 2018; Chan & Boxer Wachler 2006; Kim et al. 1998; Liu & Wang 2019; Mahr et al. 2020; Moshirfar et al. 2013; Okamoto et al. 2009; Park et al. 2012; Reinstein et al. 2013; Ru et al. 2020; Zhang et al. 2017; Zhang et al. 2020). In corneal refractive surgery, there are various recommendations from ophthalmic surgeons for centring the ablation either to the Purkinje light reflex PI originated from the corneal front surface, to the pupil centre, in between the Purkinje reflex PI and the pupil centre (Chang et al. 2016), or to the limbus (Barry & Backes 1997), in order to achieve the best visual performance after surgery. In cataract surgery, especially with premium lenses such as EDOF or multifocal designs, large angles alpha or kappa are known to have some negative impact on the prognosis for perfect visual rehabilitation, and in many articles a measurement of these angles before cataract surgery is recommended for better patient counselling or for indications for special lens designs.

In the classical definition shown in textbooks, the characteristic angles are

extracted from schematic model eyes (Chang & Waring GO 4th 2014). If, in a model eye with coaxially aligned optical elements such as in the Gullstrand or Emsley or Kooijman eye the optical axis could be defined directly as the symmetry axis of all the elements. This axis intersects all refractive surfaces of the eye perpendicularly (Chang & Waring GO 4th 2014). With an eccentric location of the fovea, the visual axis is defined as a connecting line originated from an object point to the object-side nodal point of the eye, and again a connecting line from the image-side nodal point to the fovea. Between the object-side and the image-side nodal point, the visual axis is aligned with the optical axis (Chang & Waring GO 4th 2014). In contrast, the line of sight defines the axis, which connects the object point and the centre of the entrance pupil. It is the ray, which passes through the centroid of the light bundle as a chief ray of the ray cone entering the eye. However, the line of sight does not in fact hit the fovea. The fixation axis connects the object with the centre of rotation of the eye. And last but not least, the pupil axis passes through the centre of the pupil and is perpendicular to the corneal front surface (Chang & Waring GO 4th 2014). The pupil axis hits neither the object nor the fovea.

In fact, all of these axes are imaginary: as the refractive elements of the eye in reality are not coaxially aligned, an optical axis cannot be defined. In addition, neither the visual axis, the line of sight, nor the fixation axis are measurable with any device, and the pupil axis is not really representative as an indicator for the visual performance as it is not related to the ray originated from the object passing through the eye and hitting the fovea.

The angle alpha is formed between the optical axis and the visual axis of the eye, and the angle kappa defines the angle between the pupillary axis and the visual axis measured at the centre of the entrance pupil. As the optical axis is undefined in a non-coaxial optical system and the visual axis cannot be measured, angles alpha and kappa cannot be derived by clinicians (Chang & Waring GO 4th 2014; Barragán-Garza et al. 2018).

In 2014, Chang and Waring published an article addressing this issue in detail. In response to the many inconsistencies in definitions and interpretation of these axes, they recommended the use of measures which can be derived directly from ophthalmic measurement devices in clinical use such as biometers, topographers or tomographers. All of these instruments take measures of distances or surface geometries under patient fixation with a fixation target projected to infinity to avoid instrument myopia (Chang & Waring GO 4th 2014). Chang and Waring recommended extracting the corneal outline (limbus), the outline of the entrance pupil, and the Purkinje reflex PI originated from the corneal front surface, as these measures are typically available with all of these instruments on the market. From the relative position of the Purkinje reflex PI and the centre of the pupil they defined the Chang-Waring chord (CW; Chang & Waring GO 4th 2014) in terms of vector components or as distance and direction, in order to replace the confusing terminology of angle alpha and kappa by measures, which can be taken by nearly any ophthalmic biometer or topographer on the market (Chen et al. 2011; Fişuş, Hirnschall & Findl 2021; Fişuş, Hirnschall, Ruiss et al. 2021).

The purpose of this study was to analyse the Chang-Waring chord as the distance between the Purkinje reflex PI and the entrance pupil centre before and after cataract surgery, and to build prediction models based on multilinear regression and on a neural network for estimating the postoperative CW chord from the preoperative IOLMaster 700 measurement as indicator for the visual performance after cataract surgery.

Methods

Dataset for the neural network

In total, a dataset with 19.553 data points from the IOLMaster 700 (Zeiss, Jena, Germany) from two clinical centres (Augenklinik Castrop, Germany and Kepler-University, Linz, Austria) was considered for this retrospective study (where a "data point" refers to a record of biometric measurements from an individual eye). The data were transferred to a.csv data table using the data export and backup module of the software. In the next step the tables from both clinical centres were merged. For all eyes, the respective preoperative and postoperative biometric measurements derived 5–12 weeks after cataract surgery were reorganised with all data for one eye in a single row. Data tables were reduced to the relevant parameters required for our analysis, consisting of: measurements of X/Y position of corneal centre (I_X and I_Y), X/Y position of the pupil centre (P_X and P_Y) corneal front surface curvature (flat meridian R1 with axis A1; steep meridian R2 with axis A2), axial length (AL), central corneal thickness (CCT), phakic (preoperative) or pseudophakic (postoperative) anterior chamber depth (ACD) measured from corneal front apex to the lens front apex, phakic (preoperative) or pseudophakic (postoperative) lens thickness (LT), and horizontal corneal diameter (W2W) and eye (OD/OS).

Missing data, or data with a 'Failed' or 'Warning' in the quality check for keratometry, P_X/P_Y, I_X/I_Y, AL, CCT, ACD, LT, W2W provided by the IOLMaster 700 software as well as measurements in mydriasis (pupil size > 5.5 mm) or with changes in the pupil size from preoperative to postoperative measurement of more than 1.5 mm, were excluded. After checking for 'Successful' measurement, a dataset containing records of measurements from N = 1587 eyes with preoperative and postoperative measurements was used. The data were transferred to Matlab (Matlab 2019b, MathWorks, Natick, USA) for further processing. The study was registered with the local Ethics committee (Ärztekammer des Saarlandes, 157/21).

Preprocessing of the data

Custom software was written in Matlab to calculate the Chang-Waring chord (CW_X/CW_Y) based on the offset of the entrance pupil centre (P_X and P_Y) from the X/Y position of the Purkinje reflex PI according to the method described by Chang & Waring GO 4th in 2014. From the keratometric data (K) of the corneal front surface curvature measurement (flat radius R1, axis of the flat radius A1, steep radius R2, axis of the steep radius A2), the refractive power in both cardinal meridians was derived using a keratometer index of $n_K = 1.332$, and the three vector components KEQ, $KAST_{0°}$ and $KAST_{45°}$) were calculated: the equivalent power KEQ was

extracted from the arithmetic mean of K1 = (1.332–1.0)/R1 and K2 = (1.332–1.0)/R2. The keratometric astigmatism KAST = (K2–K1) was projected to the 0°/90° axis with $KAST_{0°}$ = KAST·cos (2·A1) and to the 45°/135° axis with $KAST_{45°}$ = KAST·sin(2·A1) (Alpins & Goggin 2004). Preoperative/postoperative data were indexed with subscripts 'pre'/'post'. For further processing of the data, left eyes were mirrored as indicated by a superscript 'OD' in terms of flipping the sign of parameters with a periodicity of 360° (P_X, I_X, and CW_X) as well as flipping the sign of the oblique astigmatism vector component $KAST_{45°}$ (with a periodicity of 180°) for left eyes.

For prediction of our output parameters CW_{Xpost} and CW_{Ypost} we considered input parameters CW_X_{pre}, CW_Y_{pre}, KEQ_{pre}, $KAST_{0°pre}$, $KAST_{45°pre}$, AL_{pre}, CCT_{pre}, ACD_{pre}, LT_{pre} and $W2W_{pre}$. The dataset with N = 1587 data points was split using a random selection into a training set (70%, N = 1111) and a test set (N = 476). Both prediction models were trained with the training dataset and later validated with test dataset.

Setup of the multilinear regression model

A multivariate linear regression model was derived to predict the 2 vector components of the postoperative Chang-Waring chord, CW_{Xpost} and CW_{Ypost}, from the input parameters CW_{Xpre}, CW_{Ypre}, KEQ_{pre}, $KAST0°_{pre}$, $KAST45°_{pre}$, AL_{pre}, CCT_{pre}, ACD_{pre}, LT_{pre} and $W2W_{pre}$. A covariance-weighted least squares estimation was used, with the convergence tolerance as stopping criterion set to 1e-10. This

model output was validated against the measured Chang-Waring chord and the neural network prediction output in terms of performance with the same metric (squared prediction error) using the test data.

Setup of the neural network

A feedforward shallow multilayer multioutput neural network was set up for predicting the two vector components of the postoperative Chang-Waring chord, CW_{Xpost} and CW_{Ypost}, from the input parameters CW_{Xpre}, CW_{Ypre}, KEQ_{pre}, $KAST_{0°pre}$, $KAST_{45°pre}$, AL_{pre}, CCT_{pre}, ACD_{pre}, LT_{pre} and $W2W_{pre}$ (Zell 1994; Schmidhuber, 2015). Feedforward (in contrast to recurrent) neural networks are implementations of an artificial multilayer neural network where the nodes of a hidden layer only have connections to the subsequent hidden layer (i.e. feedforward), and do not have any feedback connections to the previous layer (s). In this context, 'shallow' refers to a neural network structure with only a few hidden layers, and 'multioutput' to the fact that more than one output value is predicted by the neural network (in our case: two vector components of CW chord), in contrast to a classical neural network with one output value. A neural network structure with two hidden layers (10 and 8 neurons, respectively), and the Levenberg-Marquardt training algorithm was selected as optimisation function (Zell 1994; Schmidhuber, 2015). Backpropagation techniques were applied for computing the gradients and Jacobian matrices and also for defining the weighting functions. The

performance of the network was evaluated with the unweighted sum of mean squared prediction error.

Validation process

Validation of our multilinear prediction model and the feedforward neural network was performed with quality metrics in terms of mean (Mean), standard deviation (SD), and median (Median) prediction error, and the 5% and 95% quantile of prediction error of both output parameters CW_{Xpost} and CW_{Ypost}. The two output parameters were compared to the Chang-Waring chord data derived from the postoperative measurement with the IOLMaster 700. The quality metrics were calculated for the test data as well as for the entire dataset.

Results

In total, our dataset consists of measurements of 798 left and 789 right eyes from 901 female and 66 male patients from two clinical centres (Castrop-Rauxel: 1094 data points, Linz: 493 data points). The mean age was 70.48 ± 9.68 years (median: 72.04 years, 90% confidence interval: 53.43–83.79 years). Table 1 shows the explorative data for the situation before cataract surgery: keratometry transformed to vector components, equivalent power KEQ, astigmatism considered on 0°/90° meridian $KAST_{0°}$ and on 45°/135° meridian $KAST_{45°}$, AL, external ACD, phakic lens thickness LT, CCT, horizontal corneal diameter W2W, the position of the pupil centre and the corneal centre with respect to the Purkinje reflex position

Table 1. Preoperative measurement data from the IOLMaster 700: KEQ, KAST0° and KAST45° refer to the vector component equivalent power and astigmatism projected to the 0°/90° and 45°/135° axis.

N = 1587	Keratometry			Distances in the eye					Pupil centre		Corneal centre		Chang-Waring chord	
	KEQ	KAST0°	KAST45°	AL	ACD	LT	CCT	W2W	P_X	P_Y	I_X	I_Y	CW_X	CW_Y
Mean	43.05	0.37	0.24	23.78	3.16	4.61	0.55	12.01	0.028	0.109	−0.006	0.131	−0.028	−0.109
SD	1.50	1.16	0.68	1.47	0.38	0.45	0.04	0.38	0.325	0.192	0.463	0.195	0.325	0.192
Median	43.08	0.37	0.02	23.55	3.17	4.60	0.55	12.00	0.030	0.106	0.077	0.133	−0.030	−0.106
5% CL	40.61	−1.33	−0.93	21.77	2.52	3.88	0.50	11.40	−0.471	−0.167	−0.634	−0.149	−0.532	−0.387
95% CL	45.55	2.42	1.04	26.51	3.77	5.35	0.62	12.65	0.532	0.387	0.618	0.407	0.471	0.167

AL, ACD, LT, CCT and W2W refer to the AL, external ACD, lens thickness, CCT and horizontal corneal diameter, P_X and P_Y refer to the X and Y coordinates of the pupil centre with respect to the Purkinje reflex PI, I_X and I_Y to the X and Y coordinates of the corneal centre with respect to the Purkinje reflex PI, and CW_X and CW_Y to the X and Y coordinates of the Chang-Waring chord defines as chord of the Pupil position with respect to the position of the Purkinje reflex PI (-P_X and -P_Y), respectively. Mean, SD, Median, 5% CL and 95% CL refer to the arithmetic mean, SD, median, 5% and 95% quantiles.
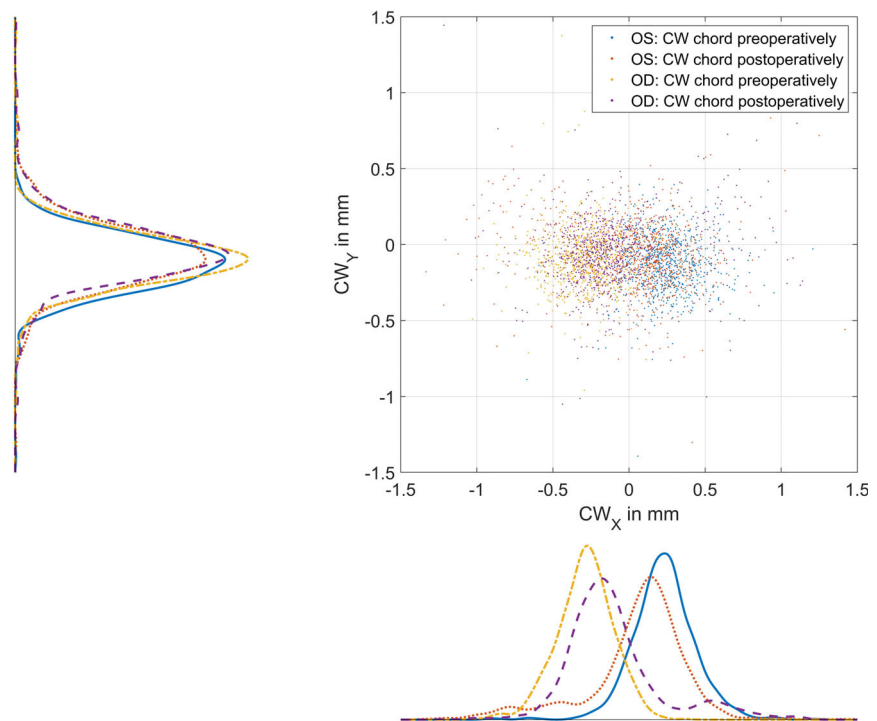
Table 2. Chang-Waring chord derived from the postoperative measurement with the IOLMaster 700, predictions of the postoperative Chang Waring chord using preoperative measurement data (keratometry, AL, external ACD, lens thickness, CCT, horizontal corneal diameter and the preoperative Chang Waring chord values) and respective prediction errors: Columns 2 and 3 refer to the measured values of the postoperative Chang-Waring chord in X and Y, columns 4 and 5 to the predictions using a multilinear regression, columns 6 and 7 to the respective prediction error; columns 8 and 9 refer to the predictions using a feedforward neural network approach, and columns 10 and 11 to the respective prediction error.

N = 1587	Chang-Waring chord measured with the IOLMaster700		Predicted Chang-Waring chord (multilinear regression)		Prediction error (multilinear regression)		Predicted Chang-Waring chord (neural network)		Prediction error (neural network)	
	CW_X^{OD}	CW_Y	CW_X^{OD}	CW_Y	CW_X^{OD}	CW_Y	CW_X^{OD}	CW_Y	CW_X^{OD}	CW_Y
Mean	−0.021	−0.060	−0.021	−0.060	0.000	0.000	−0.075	−0.060	0.000	0.000
SD	0.339	0.228	0.133	0.090	0.312	0.209	0.229	0.114	0.239	0.197
Median	−0.023	−0.067	−0.019	−0.059	−0.001	−0.009	−0.091	−0.072	−0.032	−0.003
5% CL	−0.554	0.403	−0.226	−0.194	−0.540	−0.288	−0.391	−0.238	−0.294	−0.274
95% CL	0.537	0.289	0.186	0.069	0.562	0.332	0.294	0.126	0.471	0.293

Mean, SD, Median, 5% CL and 95% CL refer to the arithmetic mean, SD, median, 5% and 95% quantiles. The X component of the Chang-Waring chord and the vector component $KAST_{45°}$ was flipped in sign for left eyes prior to consideration, in order to correspond to the conditions of right eyes.

PI, together with our target variable Chang-Waring chord defined as the position of the Purkinje reflex PI with respect to the pupil centre. For the descriptive data the 90% confidence levels are provided in addition to the arithmetic mean, the SD and the median. Table 2 shows the Chang-Waring chord derived from the postoperative measurement with the IOLMaster 700 together with the (neural network and multilinear regression based) predictions based on the preoperative measurement data (keratometry, AL, external ACD, lens thickness, CCT, horizontal corneal diameter and the preoperative Chang Waring chord values) and respective prediction errors. On average, both the multilinear regression and the neural network approach predict values for both CW chord components with a prediction error of zero. Neither the results from the neural network prediction nor those from the multilinear regression show a good performance in terms of a small prediction error compared to the target values.

Figure 1 displays the scatter and the distribution of the X and Y component of the Chang-Waring chord CW_X and CW_Y separately for left and right eyes for the preoperative and postoperative situation. The distribution of the Y components indicates that there is no variation between left and right eyes, and in both the preoperative and postoperative situation, the Purkinje reflex PI seems to be slightly inferior with respect to the pupil centre (-0.109 ± 0.192 mm and -0.060 ± 0.228 mm, respectively). However, the distributions for the X component show some differences between left (blue solid line: preoperatively; red dashed line: postoperatively) and right eyes (yellow dash-dotted line: preoperatively; purple dashed line: postoperatively; both with negative CW_X values), as well as differences between the preoperative and postoperative

Fig. 1. Combined scatterplot and histogram of the Chang-Waring chord measurements of the IOLMaster 700 for the preoperative and postoperative situation grouped for eye side (left eyes: OS, right eyes: OD). The distribution for the Y component shows slightly negative values (Purkinje reflex PI inferior to the pupil centre) and does not differ for left and right eyes and for the preoperative and postoperative situation. The X component preoperatively and postoperatively a systematic shift of the Purkinje reflex PI to temporally (positive values for left and negative values for right eyes), where preoperative values tend to be located more temporally than postoperatively but with narrower distributions.

situation: there is a systematic shift of the distributions in the temporal direction (with positive CW_X values for the left and negative values for the right eye), which is more pronounced preoperatively than postoperatively (the distributions for the left eye (solid blue line) and right eye (dash-dotted yellow line both
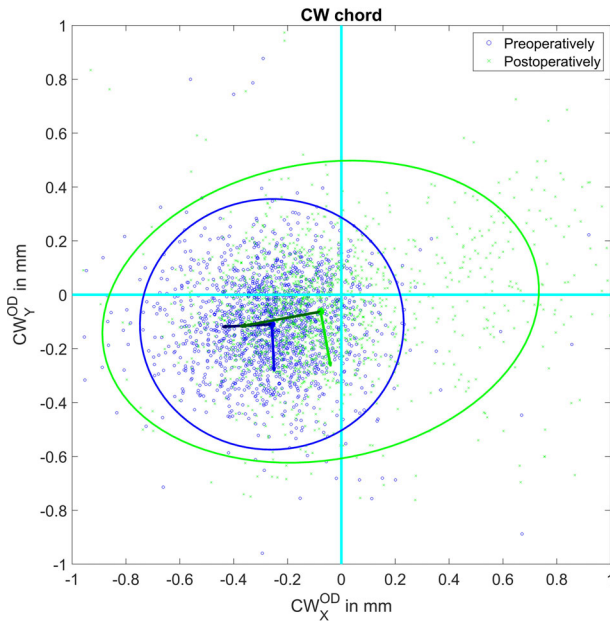
Fig. 2. Preoperative and postoperative Chang-Waring chord (CW chord) derived from the IOLMaster 700 measurement. The CW chord shows the relative position of the Purkinje I image from the pupil centre. The blue and green ellipses refer to the 95% confidence ellipses for the preoperative and postoperative situations. The dark blue and light blue vectors indicate the eigenvalues of the covariance matrix (orientation of the ellipse with the major and minor axes) for the preoperative situation, and the dark green and light green vectors refer to the eigenvalues of the covariance matrix (orientation of the ellipse with the major and minor axes) for the postoperative situation. The X component of the Chang-Waring chord was flipped in sign for left eyes prior to consideration to mimic the conditions of right eyes (indicated by a superscript 'OD').

shift towards the y axis from preoperatively to postoperatively (red dotted line and purple dashed line)). Postoperatively, the distributions appear to be flatter for both left and right eyes, which indicate that there is more variation in the X component of the CW chord postoperatively. In addition, the distributions postoperatively are somewhat asymmetric where some eyes show negative/positive values for CW_X for the left/right eye.

Figure 2 shows the scatterplot of the X and Y component of the Chang-Waring chord for the situation before and after cataract surgery with the measurements corrected for right eyes (the X component of the CW chord is flipped in sign for left eyes). Again, we see a much higher concentration of the values prior to cataract surgery (blue dots) compared to postoperatively (green dots) (smaller confidence ellipse preoperatively (blue ellipse) compared to postoperatively (green ellipse)). The respective centres of the ellipses (centre in X/Y direction: −0.26/−0.11 mm preoperatively and −0.08/−0.06 mm) are shown with a blue and green marker. The Purkinje reflex seems to be on average inferior (lower half of the

plot) and temporal (left half of the plot) to the pupil centre, more in the preoperative than in the postoperative measurement. In the preoperative situation, the confidence ellipse (blue ellipse, major half axis 0.49 mm at 3°, minor half axis 0.47 mm at 93°) is smaller compared to the postoperative situation (green ellipse, major half axis 0.82 mm at 10°, minor half axis 0.55 mm at 100°) and the aspect ratio of the ellipse is smaller (1.05 versus 1.49). In Fig. 3, the change in CW chord from the preoperative to the postoperative situation is shown. The Purkinje reflex PI systematically shifts in the superior (0.05 mm) and nasal (0.18 mm) directions, but with a large scatter as indicated by the 90% confidence ellipse (major half axis 0.79 mm at 9°, minor half axis 0.57 mm at 99°, aspect ratio 1.39).

Figure 4 displays the results of the multilinear prediction model and the feedforward neural network prediction model in forecasting the postoperative Chang-Waring chord from the preoperative biometric measurement data and the preoperative CW chord. From the wide scatter of data, we see that prediction performance of both models

is not satisfactory: especially for the X component (left graph) the prediction systematically underestimates the CW chord measured postoperatively with the IOLMaster 700. Especially for the multilinear but also for the neural network based prediction, the ellipses are flatter compared to the cyan reference line. Also, for the Y component the prediction models underestimate the postoperative CW chord (as indicated by ellipses with orientations flatter than the cyan reference line), although the scatter is significantly less compared to the X component. The respective ellipses are for the X component (left graph, multivariate linear regression model: centre of the ellipse in X/Y direction: −0.08/−0.08 mm, major half axis 0.87 mm at 22°, minor half axis 0.18 mm at 112°, aspect ratio 4.89; feedforward neural network: centre of the ellipse in X/Y direction: −0.08/−0.08 mm, major half axis 0.97 mm at 35°, minor half axis 0.23 mm at 125°, aspect ratio 4.12), and for the Y component (multivariate linear regression model: centre of the ellipse in X/Y direction: −0.06/−0.06 mm, major half axis 0.61 mm at 23°, minor half axis 0.13 mm at 113°, aspect ratio 4.68; feedforward neural network: centre of the ellipse in X/Y direction: −0.06/−0.06 mm, major half axis 0.62 mm at 27°, minor half axis 0.15 mm at 117°, aspect ratio 4.15).

Discussion

There is plenty of scientific discussion regarding the impact of angle alpha or kappa on the prognosis of corneal refractive procedures (Arba Mosquera et al. 2015; Chan & Boxer Wachler 2006; Kim et al. 1998; Liu & Wang 2019; Moshirfar et al. 2013; Okamoto et al. 2009; Park et al. 2012; Reinstein et al. 2013; Ru et al. 2020; Zhang et al. 2017; Zhang et al. 2020), and also on corneal inlays (Barragán-Garza 2018) or cataract surgery (Mahr et al. 2020), especially with premium lenses. Definitions of these angles in the literature are often confusing, and ultimately these angles cannot be defined or measured in a real patient's eye as there is no clearly defined reference axis (Chang & Waring GO 4th 2014). For the angle alpha, we require the optical axis, which is generally not defined in non-coaxial optical systems. In
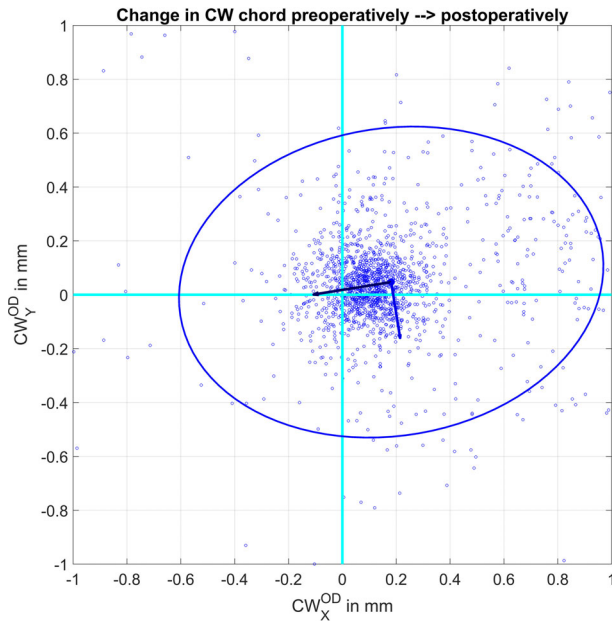
Fig. 3. Change of Chang-Waring chord (CW chord) derived from the IOLMaster 700 measurement from the preoperative to the postoperative situation. The CW chord shows the relative position of the Purkinje I image from the pupil centre. The blue ellipse refers to the 95% confidence ellipse. The dark blue and light blue vectors indicate the eigenvalues of the covariance matrix (orientation of the ellipse with the major and minor axes). The X component of the Chang-Waring chord was flipped in sign for left eyes prior to consideration to mimic the conditions of right eyes (indicated by a superscript 'OD'). Due to cataract surgery the Purkinje reflex PI shifts systematically towards the centre (to the superior and nasal direction).

addition, the visual axis cannot be derived from the measurement. For the angle kappa, even if the pupillary axis could be extracted from tomographic measurements of the anterior eye segment, the visual axis cannot be measured with any device.

Therefore, Chang and Waring recommended in their article from 2014 to use distances, which can be directly obtained using optical measurement tools that measure with a coaxial fixation light, and this parameter was named the Chang-Waring chord (Chang & Waring GO 4th 2014). In general, all topographers, tomographers or optical biometers measure distances or curvatures under the patient's fixation, and therefore such parameters can be directly extracted from the measurement by processing the pupil outline and the Purkinje reflex PI originated from the corneal front surface. Furthermore, the relative position of the Purkinje reflex to the corneal centre may give additional insight, for example, for a limbus centration of a refractive procedure (Barry & Backes 1997).
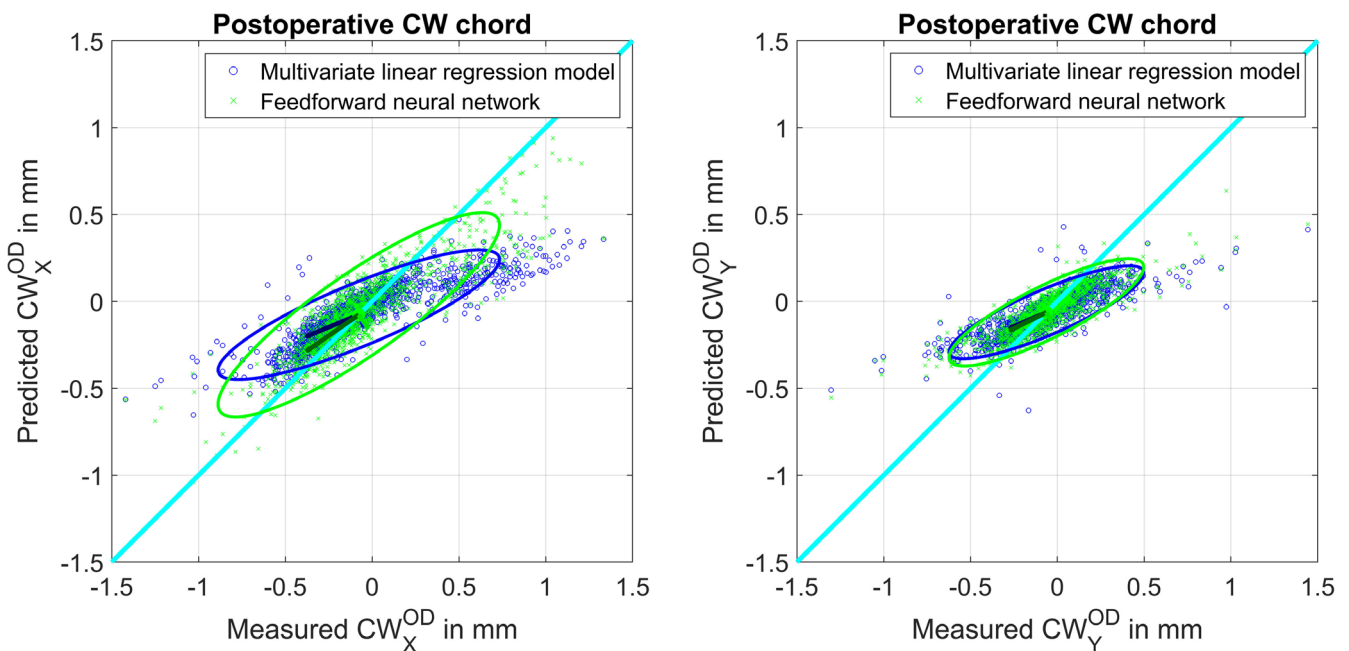
Fig. 4. Predicted postoperative Chang-Waring chord (CW chord) versus postoperative CW chord derived from the postoperative measurement with the IOLMaster 700 for the X component (left image) and the Y component (right image). Prediction was performed with a multilinear regression approach (blue) and with a feedforward neural network approach (green). The prediction of the X component of CW chord seems to be worse for both prediction methods (larger 95% confidence ellipses for the X component on the left graph; blue ellipse: multilinear regression and green: neural network) compared to the Y component (blue and green ellipse on the right graph). The dark blue/dark green vectors on both graphs refer to the larger eigenvalues of the covariance matrix (indicating the orientation of the ellipse), and the light blue and light green vectors to the smaller eigenvalues. Values located on the cyan line refer to a match between prediction and measurements. The X component of the Chang-Waring chord was flipped in sign for left eyes prior to consideration to mimic the conditions of right eyes (indicated by a superscript 'OD').

We should be aware that the Purkinje light reflex PI is not formed at the corneal front surface, but (for a coaxial light source located at infinity) at half the distance between the intersection of the blue line with the cornea and the centre of the corneal front surface curvature (around 3.85 mm behind the front surface). Therefore, the CW chord cannot be directly translated into angle alpha or kappa, as both the location of the fixation light and the corneal curvature affect the chord. In addition, as the centre of the pupil is known to change with the pupil size (Erdem et al. 2008) there might be some additional uncertainty of the chord with pupil size. Nevertheless, the major benefit of this chord compared to classical definitions of angle alpha or kappa is that the measurement is nearly independent of the measurement device as long as a coaxial light source at far distance is used. Therefore, it is important for the clinician to differentiate between the apparent CW chord and the actual chord μ, which refers to the chord length between either the Purkinje image PI and the apparent pupil centre viewed coaxially from a light source through the cornea or the actual distance from the visual axis and the actual pupil centre (Holladay 2019). The apparent pupil is magnified and displaced by the cornea, therefore the apparent CW chord is larger than the actual chord μ and does not directly translate to angle kappa, but is dependent on actual chord length, corneal power and ACD (Holladay 2019). As a rule of thumb and without taking AL into consideration, a chord length of 1.0 mm refers to an angle kappa of around 7.5° (Holladay 2019). While optical biometry and topography typically display the apparent CW chord, Scheimpflug tomography and OCT usually display the actual chord μ (Jiang et al. 2020). Normative values for the CW chord are 0.34 ± 0.16 mm. We observed a mean CW chord of 0.348 ± 0.183/ 0.339 ± 0.235 mm before/after cataract surgery. Normative values for angle kappa differ with AL and range from 1.74° (myopic) to 3.84° (hyperopic) when measured with a synoptophore (Basmak et al. 2007).

Based on measurements of the CW chord, Prakash et al. (2011) found correlations between large chords and the degree of severity of photic phenomena after multifocal lens implantation. A large angle kappa may be linked to coma-like aberrations, which themselves may accelerate the occurrence of photic phenomena (Braga et al. 2014). Standard screening for angle kappa before multifocal IOL insertion has been recommended. For indication of multifocal intraocular lenses, surgeons should be careful with large values (e.g. >0.6 mm or the radius of the inner diffractive structure) in order to prevent light rays from passing through the multifocal ring segments (Holladay 2019; Espaillat et al. 2021).

However, The CW chord does not solve all problems with centring the ablation in corneal refractive procedures, centring corneal inlays or for indication of premium intraocular lenses. Even if the location of the Purkinje reflex PI is largely unaffected by the pupil size at least under photopic or mesopic light conditions, the distance of the Purkinje reflex PI relative to the pupil centre does change with the light conditions (photopic/ mesopic/scotopic light conditions: 0.19/0.23/0.24 mm; Yang et al. 2002). As there is no significant correlation between the Purkinje reflex PI position and age, refraction, corneal diameter, or pupil diameter, this parameter seems to be appropriate as a landmark or reference for the centre of corneal curvature. The pupil centre is typically decentred in the nasal direction and slightly in the superior direction (Yang et al. 2002), which is in accordance to our results with a CW chord having a temporal-inferior shift on average.

In this article, we have attempted to extract the Chang-Waring chord from the X and Y positions of the pupil centre and the Purkinje light reflex PI in a large population of cataract patients with biometric measurements prior to and after cataract surgery. We discovered that the Purkinje reflex PI is slightly shifted in the inferior direction (negative Y coordinate) in the preoperative as well as in the postoperative situation. In the horizontal direction (X coordinate), we observed symmetry between left and right eyes with a systematic shift of the Purkinje reflex PI in the temporal direction, but with a wide scatter. Preoperatively, the Purkinje reflex image PI is located more temporally compared to postoperatively, and postoperatively it shows even more scatter compared to preoperatively. As a result of cataract surgery, we observed on average a superior-nasal shift, but with a large scatter to both directions. As it has been discussed in the literature that the angles alpha and kappa may play a major role in the prognosis of corneal refractive surgery and cataract procedures especially with premium lenses, we tried to derive a prediction strategy for the postoperative CW chord following cataract surgery from the CW chord prior to cataract surgery (CW_X and CW_Y), the vector components of keratometry (KEQ, $KAST_{0°}$, $KAST_{45°}$) and several biometric measures grabbed in a routine pre-cataract biometric measures, such as AL, ACD, phakic lens thickness, CCT, and the horizontal corneal diameter. However, our prediction approach with a multilinear regression and also with a feed-forward neural network having two output parameters and 10 input parameters does not yield convincing results. This suggests that a prediction with the clinically required precision does not seem to be possible with the 10 effect sizes that were used in our setting. Ultimately, the variance of the prediction error for the X component of CW chord (compare SD in Table 2) is only slightly smaller with 0.097/0.044 mm² for the multilinear regression approach and 0.057/0.039 mm² compared to the variance of the CW chord derived from the IOLMaster 700 measurement after cataract surgery (0.115/0.052 mm²).

As clinical consequence, a prediction of Chang-Waring chord values after cataract surgery with the 10 effect sizes derived from the preoperative biometric measurement as used in our setting does not yield sufficient precision. If we assume that the CW chord shows some predictive value for the outcome after cataract surgery in terms of visual performance, other techniques would need to be applied to predict the CW chord for the postoperative situation from preoperative measurement data available from standard biometry for lens power calculation prior to cataract surgery.

In conclusion, with modern optical biometers, topographers or tomographers that measure distances or surface shape under fixation with a coaxial fixation light, the position of the entrance pupil centre and the Purkinje reflex PI can be directly measured nearly independent of the device. In

contrast to the angle alpha and kappa, which have been widely discussed in recent years for potential impact on the functional result after corneal refractive surgery or cataract surgery, the CW chord defined as Purkinje reflex PI position with respect to the entrance pupil centre can be directly measured. This CW chord is affected by corneal curvature and pupil size. In a cataract population, a prediction for the post-operative CW chord from the preoperative chord, keratometry and biometric distances derived from preoperative biometry seems to be unreliable due to a large scatter in the data.

References

Alpins NA & Goggin M (2004): Practical astigmatism analysis for refractive outcomes in cataract and refractive surgery. Surv Ophthalmol 49: 109–122. https://doi.org/10.1016/j.survophthal.2003.10.010.

Arba Mosquera S, Verma S & McAlinden C. (2015): Centration axis in refractive surgery. Eye vis (Lond) 2: 4. https://doi.org/10.1186/s40662-015-0014-6.

Barragán-Garza E, Koch DD, Vargas LG, Lang A & Roy A. (2018): The sensitivity of clinical outcomes to centration on the light-constricted pupil for a shape-changing corneal inlay. J Refract Surg 34: 164–170. https://doi.org/10.3928/1081597X-20180103-02.

Barry JC & Backes A. (1997): Limbus versus pupil center for ocular alignment measurement with corneal reflexes. Invest Ophthalmol vis Sci 38: 2597–2607.

Basmak H, Sahin A, Yildirim N, Papakostas TD & Kanellopoulos AJ. (2007): Measurement of angle kappa with synoptophore and Orbscan II in a normal population. J Refract Surg 23: 456–460. PMID: 17523505.

Braga-Mele R, Chang D, Dewey S et al. (2014): Multifocal intraocular lenses: relative indications and contraindications for implantation. J Cataract Refract Surg 40: 313–322. https://doi.org/10.1016/j.jcrs.2013.12.011.

Chan CC & Boxer Wachler BS. (2006): Centration analysis of ablation over the coaxial corneal light reflex for hyperopic LASIK. J Refract Surg 22: 467–471.

Chang DH & Waring GO 4th. (2014): The subject-fixated coaxially sighted corneal light reflex: a clinical marker for centration of refractive treatments and devices. Am J Ophthalmol 158: 863–874. https://doi.org/10.1016/j.ajo.2014.06.028.

Chang JS, Law AK, Ng JC & Chan VK. (2016): Comparison of refractive and visual outcomes with centration points 80% and 100% from pupil center toward the coaxially sighted corneal light reflex. J Cataract Refract Surg 42: 412–419. https://doi.org/10.1016/j.jcrs.2015.09.030.

Chen YA, Hirnschall N & Findl O. (2011): Evaluation of 2 new optical biometry devices and comparison with the current gold standard biometer. J Cataract Refract Surg 37: 513–517. https://doi.org/10.1016/j.jcrs.2010.10.041.

Erdem U, Muftuoglu O, Gündogan FC, Sobaci G & Bayer A. (2008): Pupil center shift relative to the coaxially sighted corneal light reflex under natural and pharmacologically dilated conditions. J Refract Surg 24: 530–538. https://doi.org/10.3928/1081597X-20080501-12.

Espaillat A, Coelho C, Medrano Batista MJ & Perez O. (2021): Predictors of photic phenomena with a trifocal IOL. Clin Ophthalmol 15: 495–503. https://doi.org/10.2147/OPTH.S282469.

Fişuş AD, Hirnschall ND & Findl O. (2021): Comparison of two swept-source optical coherence tomography-based biometry devices. J Cataract Refract Surg 47: 87–92. https://doi.org/10.1097/j.jcrs.0000000000000373.

Fişuş AD, Hirnschall ND, Ruiss M, Pilwachs C, Georgiev S & Findl O. (2021): Repeatability of two swept-source optical coherence tomography biometers and one optical low coherence reflectometry biometer. J Cataract Refract Surg 47: 1302–1307. https://doi.org/10.1097/j.jcrs.0000000000000633.

Holladay JT. (2019): Apparent chord mu and actual chord mu and their clinical value. J Cataract Refract Surg 45: 1198–1199. https://doi.org/10.1016/j.jcrs.2019.03.029.

Jiang JY, Hodge C & Lawless M. (2020): Understanding chord mu through a large population-based study. Clin Exp Ophthalmol 48: 998–1001. https://doi.org/10.1111/ceo.13800.

Kim EK, Jang JW, Lee JB, Hong SB, Lee YG & Kim HB. (1998): Comparison of corneal centering in photorefractive keratectomy. Yonsei Med J 39: 317–321. https://doi.org/10.3349/ymj.1998.39.4.317.

Liu Y & Wang Y. (2019): Optical quality comparison between laser ablated myopic eyes with centration on coaxially sighted corneal light reflex and on entrance pupil center. J Opt Soc Am A 36: B103–B109. https://doi.org/10.1364/JOSAA.36.00B103.

Mahr MA, Simpson MJ & Erie JC. (2020): Angle alpha orientation and magnitude distribution in a cataract surgery population. J Cataract Refract Surg 46: 372–377. https://doi.org/10.1097/j.jcrs.0000000000000066.

Moshirfar M, Hoggan RN & Muthappan V. (2013): Angle Kappa and its importance in refractive surgery. Oman J Ophthalmol 6: 151–158. https://doi.org/10.4103/0974-620X.122268.

Okamoto S, Kimura K, Funakura M, Ikeda N, Hiramatsu H & Bains HS. (2009): Comparison of Myopic LASIK Centered on the Coaxially Sighted Corneal Light Reflex or Line of Sight. J Refract Surg 25(10 Suppl): S944–S950. https://doi.org/10.3928/1081597X-20090915-09.

Park CY, Oh SY & Chuck RS. (2012): Measurement of angle kappa and centration in refractive surgery. Curr Opin Ophthalmol 23: 269–275. https://doi.org/10.1097/ICU.0b013e3283543c41.

Prakash G, Prakash DR, Agarwal A, Kumar DA, Agarwal A & Jacob S. (2011): Predictive factor and kappa angle analysis for visual satisfactions in patients with multifocal IOL implantation. Eye 25: 1187–1193. https://doi.org/10.1038/eye.2011.150.

Reinstein DZ, Gobbe M & Archer TJ. (2013): Coaxially sighted corneal light reflex versus entrance pupil center centration of moderate to high hyperopic corneal ablations in eyes with small and large angle kappa. J Refract Surg 29: 518–525. https://doi.org/10.3928/1081597X-20130719-08.

Ru XY, Li ZR, Li CL, Cui H, Deng WQ, Lin SH, Jia YJ & Li YJ. (2020): Correlation analysis of refractive and visual quality after wavefront-optimized laser in situ keratomileusis for 50% and 100% angle kappa compensation. J Ophthalmol 2020: 9873504. https://doi.org/10.1155/2020/9873504.

Schmidhuber J (2015): Deep learning in neural networks: An overview. Neural Networks 61: 85–117. https://doi.org/10.1016/j.neunet.2014.09.003.

Yang Y, Thompson K & Burns SA. (2002): Pupil location under mesopic, photopic, and pharmacologically dilated conditions. Invest Ophthalmol vis Sci 43: 2508–2512.

Zell A (1994): Simulation Neuronaler Netze [Simulation of Neural Networks]., 1st edn. Boston, USA: Addison-Wesley, 73.

Zhang J, Wang Y, Chen X & Wu W. (2020): Clinical outcomes of corneal refractive surgery comparing centration on the corneal vertex with the pupil center: a meta-analysis. Int Ophthalmol 40: 3555–3563. https://doi.org/10.1007/s10792-020-01506-1.

Zhang J, Zhang SS, Yu Q & Lian JC. (2017): Comparison of visual effects of FS-LASIK for myopia centered on the coaxially sighted corneal light reflex or the line of sight. Int J Ophthalmol 10: 624–631. https://doi.org/10.18240/ijo.2017.04.20.

Correspondence:
Prof. Dr. Achim Langenbucher
Department of Experimental Ophthalmology
Saarland University
Kirrberger Str 100 Bldg. 22
66424 Homburg, Germany
Tel: +49 6841 1621218
Fax: +49 6841 1621240
Email: achim.langenbucher@uks.eu